

Substituted 4-Carboxymethylpyroglutamic Acid Diamides as Potent and Selective Inhibitors of Fibroblast Activation Protein

Ting-Yueh Tsai,[†] Teng-Kuang Yeh,[†] Xin Chen,[†] Tsu Hsu, Yu-Chen Jao, Chih-Hsiang Huang, Jen-Shin Song, Yu-Chen Huang, Chia-Hui Chien, Jing-Huai Chiu, Shih-Chieh Yen, Hung-Kuan Tang, Yu-Sheng Chao, and Weir-Torn Jiaang*

Division of Biotechnology and Pharmaceutical Research, National Health Research Institutes, No. 35, Keyan Road, Zhunan Town, Miaoli Country 350, Taiwan, R.O.C. [†]These authors contributed equally to this work.

Received February 26, 2010

Fibroblast activation protein (FAP) belongs to the prolyl peptidase family. FAP inhibition is expected to become a new antitumor target. Most known FAP inhibitors often resemble the dipeptide cleavage products, with a boroproline at the P1 site; however, these inhibitors also inhibit DPP-IV, DPP-II, DPP8, and DPP9. Potent and selective FAP inhibitor is needed in evaluating that FAP as a therapeutic target. Therefore, it is important to develop selective FAP inhibitors for the use of target validation. To achieve this, optimization of the nonselective DPP-IV inhibitor **8** led to the discovery of a new class of substituted 4-carboxymethylpyroglutamic acid diamides as FAP inhibitors. SAR studies resulted in a number of FAP inhibitors having IC₅₀ of < 100 nM with excellent selectivity over DPP-IV, DPP-II, DPP8, and DPP9 (IC₅₀ > 100 μM). Compounds **18a**, **18b**, and **19** are the only known potent and selective FAP inhibitors, which prompts us to further study the physiological role of FAP.

Introduction

Fibroblast activation protein (FAP^a) is a type II transmembrane serine protease belonging to the prolyl peptidase family, which comprises serine proteases that cleave bioactive peptides preferentially after proline residues. Members of this family include dipeptidyl peptidase-IV (DPP-IV), DPP-II (DPP7), DPP8, and DPP9, and this family has been implicated in several diseases, including diabetes, cancer, and mood disorder.^{1,2} FAP is expressed on reactive stromal fibroblasts in over 90% of common human epithelial cancers,³ in granulation tissue of healing wounds, and in bone and soft tissue sarcomas.^{4,5} It has been suggested that FAP promotes tumorigenesis and that FAP inhibition may attenuate tumor growth.^{6–8} The development of potent and specific inhibitors for each of these DPP enzymes can be an important tool to study the physiological function and to validate their potential as a therapeutic target. Specific inhibitors for DPP-IV,^{9–11} DPP-II,^{12,13} and DPP8/9¹⁴ have been identified, and investigations of selective inhibitors for FAP have only started recently.^{15–17}

Dipeptidyl peptidase IV (DPP-IV, also known as CD26) (EC 3.4.14.5) is a drug target for type II diabetes. The active form of glucagon-like peptide-1 (GLP-1) stimulates insulin secretion, inhibits glucagons release,^{18,19} and slows gastric emptying,^{20–22} each a benefit in the control of glucose homeostasis

in patients with type 2 diabetes.^{23,24} Therefore, inhibition of DPP-IV prolongs the action of GLP-1, which offers a new strategy for treating type 2 diabetes. Antidiabetic efficacy has been demonstrated clinically with DPP-IV inhibitors; sitagliptin **1** (MK-0431) was approved by the U.S. Food and Drug Administration for the treatment of type 2 diabetes,¹⁰ and vildagliptin **2** (LAF237) was approved for use in the European market (Figure 1).⁹

Dipeptidyl peptidase II (DPP-II, EC 3.4.14.2) is believed to be involved in the physiological breakdown of some proline-containing neuropeptides and in the degradation of collagen and substance P.^{25,26} Using 1-[(S)-2,4-diaminobutanoyl]piperidine as lead compound, Senten et al. developed a series of potent and selective DPP-II inhibitors.^{12,13} The representative DPP-II inhibitor **3** (Figure 1) showed IC₅₀ = 0.23 nM and a high selectivity toward DPP-IV (IC₅₀ = 345 μM, Table 1).¹³ Our studies found that compound **3** was inactive toward FAP, DPP8, and DPP9 (Table 1). These selective DPP-II inhibitors are outstanding tools to determine the physiological function of DPP-II and the therapeutic potential of DPP-II inhibitors.

Dipeptidyl peptidase 8/9 (DPP8/9) are cytoplasmic proteases with a 51% homology in amino acid level with DPP-IV.²⁷ Previously, the administration of selective DPP8/9 inhibitor **4** (Figure 1) may be associated with profound toxicities in preclinical species, which included alopecia, thrombocytopenia, anemia, enlarged spleen, multiple histological pathologies, and animal mortality shown in rats.²⁸ Highly specific and potent DPP8/9 inhibitors were also developed by Jiaang et al. The representative DPP8/9 inhibitor **5** (also called 1G-244, Figure 1) had IC₅₀ values of 14 and 53 nM against DPP8 and DPP9, respectively (Table 1).¹⁴ It did not inhibit DPP-IV, FAP, or DPP-II, with IC₅₀ values greater than 100 μM. Recently, by using this potent and selective DPP8/9 inhibitor,

*To whom correspondence should be addressed. Phone: 886-37-246166, extension 35712. Fax: 886-37-586456. E-mail: wtjiaang@nhri.org.tw.

^a Abbreviations: FAP, fibroblast activation protein; DPP, dipeptidyl peptidase; GLP-1, glucagon-like peptide-1; LiHMDS, lithium hexamethyldisilazide; DBU, 1,8-diazabicyclo[5.4.0]undec-7-ene; EDC, 1-ethyl-3-(3-dimethylaminopropyl)carbodiimide; TFA, trifluoroacetic acid; LC-MS, liquid chromatography coupled mass spectrometry; SAR, structure-activity relationship; HOBt, *N*-hydroxybenzotriazole.

Wu et al. show that the inhibition is not associated with any animal toxicity.²⁹

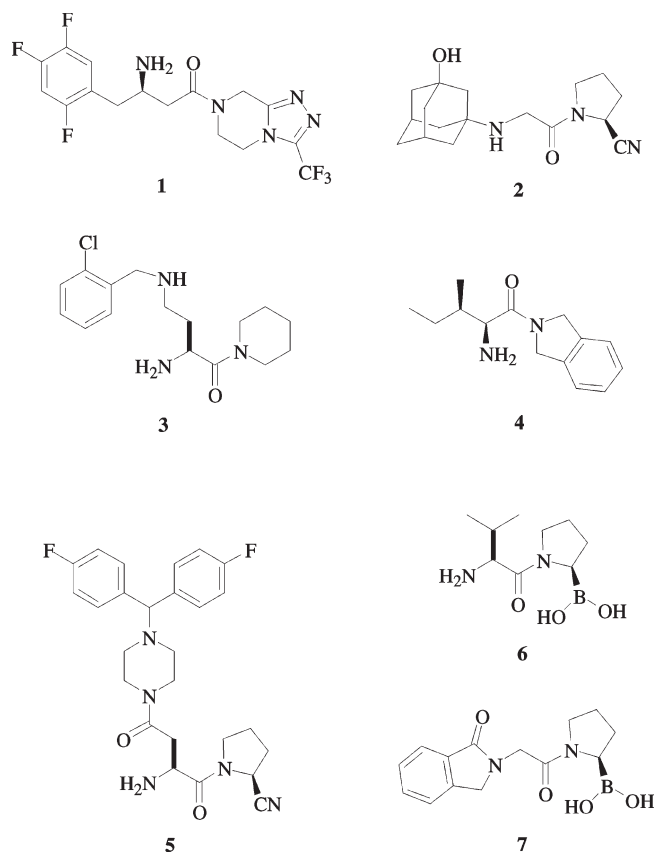


Figure 1. DPP-IV inhibitors **1** and **2**, DPP-II inhibitor **3**, DPP8/9 inhibitors **4** and **5**, nonselective inhibitor **6**, and FAP inhibitor **7**.

Table 1. Potency and Selectivity of Compounds 1–8

compd	name	IC ₅₀ (μM) ^a					reference ^b
		FAP	DPP8	DPP9	DPP-II	DPP-IV	
1	sitagliptin	> 100	> 100	> 100	> 100	0.023	this study
2	vildagliptin	> 100	14	1.2	> 50	0.056	this study
3	DPP-II selective	ND	ND	ND	0.00023	345	13
4	DPP8/9 selective	> 100	> 100	> 100	0.005	> 100	this study
5	1G-244	> 100	0.15	0.24	> 100	> 100	this study
6	nonselective	> 100	0.014	0.053	> 100	> 100	this study
7	FAP selective	0.011	ND	ND	0.038	0.0003	15
8	1G-409	0.008	ND	ND	ND	23	16
		0.12	11	6.5	> 100	8.0	this study
		0.054	0.36	0.089	2.6	0.010	this study

^aMean values of at least three experiments; standard deviations are ±20%. ND, no data. ^b“This study” means in-house data.

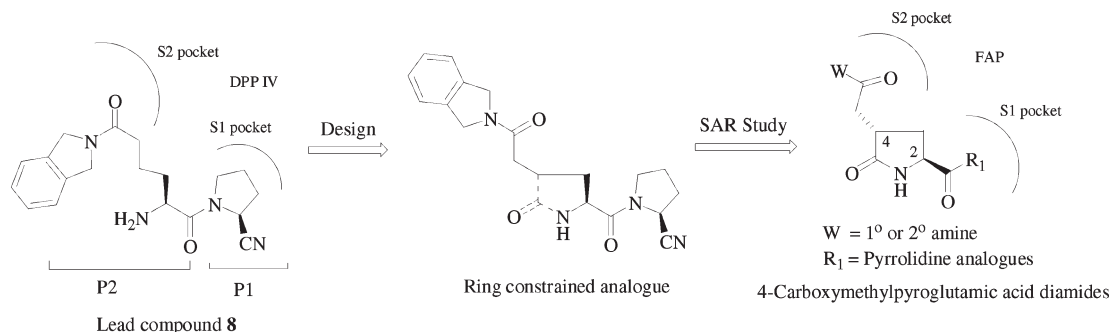


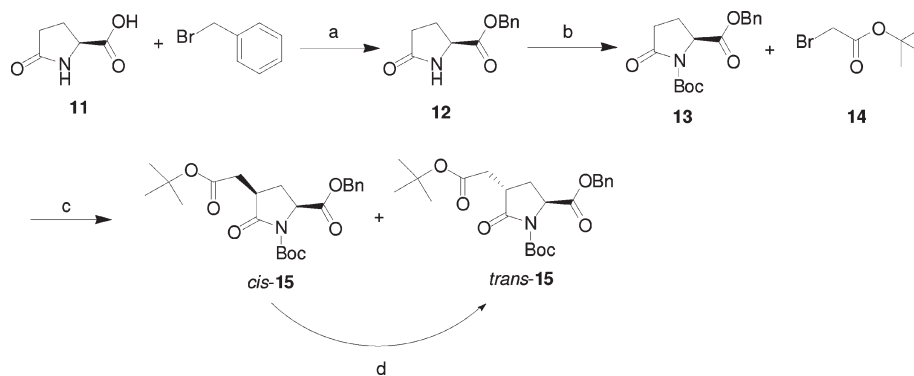
Figure 2. Design of 4-carboxymethylpyroglutamic acid diamides as FAP inhibitors.

Previously, N- and αC-substituted Gly-boro-Pro derivatives have been developed, and these compounds strongly inhibited DPP-IV, DPP7 (DPP-II), and FAP. In this class, a representative compound is Val-boroPro **6** (Figure 1), having IC₅₀ of < 40 nM against all the three DPPs (Table 1).¹⁵ On the basis of FAP's preference for Gly-Pro-based endopeptidase substrates, Tran et al. developed a series of N-acyl-Gly-, N-acyl-Sar- (sarcosine), and N-blocked-boroPro derivatives. Representative compound in this class was inhibitor **7** (Figure 1), which preferentially inhibited FAP versus DPP-IV, but the selectivity against DPP-II, DPP8, and DPP9 was not reported (Table 1).¹⁶ In our studies, this compound had weak inhibitory activity against DPP8 and DPP9 (11 and 6.5 μM, respectively) and was inactive toward DPP-II (Table 1).

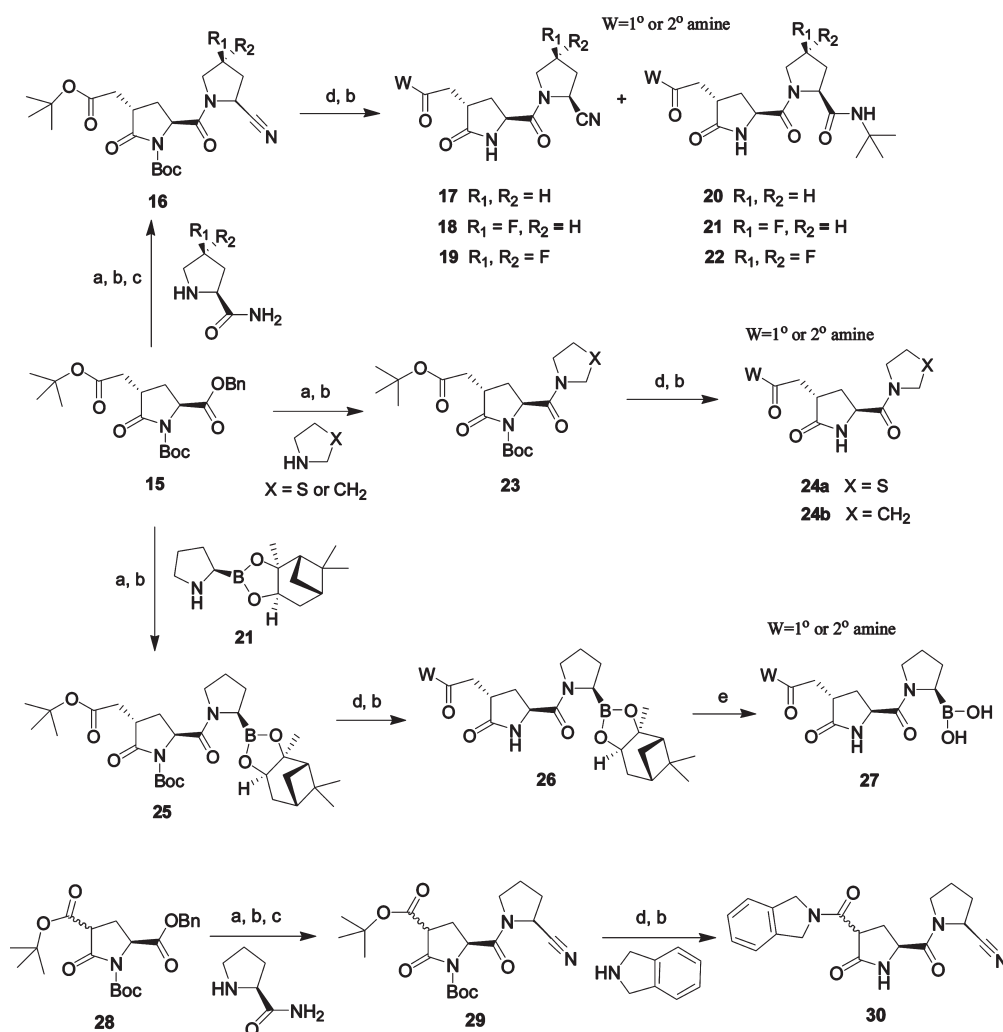
In this paper, we report a systematic search for potent and selective FAP inhibitors. A structure–activity relationship was investigated starting from L-homoglutamic acid **8** (Figure 2), a dual DPP-V and FAP inhibitor (IC₅₀ = 10 and 54 nM, respectively), as a lead compound (Table 1).³⁰ To develop selective FAP inhibitors, introduction of ring constraint in the P2 portion of lead **8** and modification of the P2 site secondary amine to amide were done as depicted in Figure 2. The replacement of secondary amine with amide is based on the fact that FAP acts as both prolin-specific endopeptidase and dipeptidyl peptidase, but DPP-IV prefers to display the latter activity.^{8,16,31} Further exploration of the 2-position pyrrolidine derivatives (P1 site) and the 4-position amine substituents at the carbonylmethyl group (P2 site) led to the discovery of potent pyroglutamic acid-based FAP inhibitors with a high selectivity for FAP over DPP-IV, DPP-II, DPP8, and DPP9.

Chemistry

Reference compounds N-acyl-Gly-boroPro **9** and N-acyl-Gly-cyanoPro **10** were prepared according to the literature

Scheme 1. Synthesis of C(4)-Substituted Pyroglutamate Ester Urethanes^a

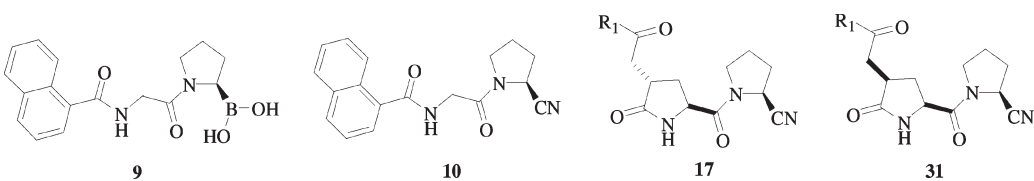
^a Reagents: (a) DIEPA, CH₂Cl₂; (b) (Boc)₂O, 4-DMAP, CH₂Cl₂; (c) LiHMDS, THF, -78 °C; (d) DBU, CH₂Cl₂, 0 °C to room temp.

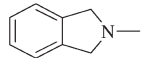
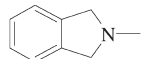
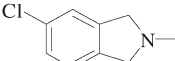
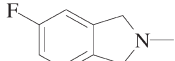
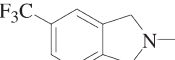
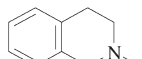
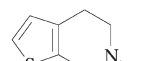
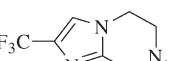
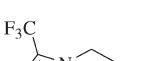
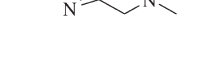
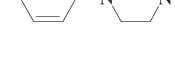
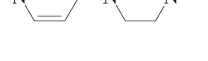
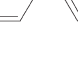
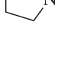
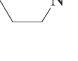
Scheme 2. Synthesis of FAP Inhibitors 17–22, 24, 27, and 30^a

^a Reagents: (a) H₂, Pd/C, MeOH; (b) EDC, HOBT, CH₂Cl₂/1,4-dioxane, various amines; (c) POCl₃, imidazole, pyridine; (d) TFA, CH₃CN, 0 °C to room temp; (e) BCl₃.

procedures with some modifications.^{9,16} (2*S*)-Cyanopyrrolidine analogues **17–19**, **24**, **27**, **30**, and **31** were prepared as described in Schemes 1 and 2 and are listed in Tables 2 and 3. The synthesis (Scheme 1) proceeded in good yield following the procedure of Young and co-workers to afford the fully protected pyroglutamate **13**.³² The stereoselective alkylation using lithium hexamethyldisilazide (LiHMDS) and *tert*-butyl bro-

moacetate **14** gave compound **15** in 70% yield with a *cis/trans* ratio of 3:1. The *cis* isomer **15** was treated with 1,8-diazabicyclo[5.4.0]undec-7-ene (DBU) in methylene chloride for 24 h to give inverted product in a 1:3 ratio and high yield. The assignment of the *cis/trans* configuration was based on the results reported in the literature.^{33,34} By use of the building block of C(4)-substituted pyroglutamate ester urethanes *cis*- and *trans*-**15**,

Table 2. Inhibition of FAP, DPP-IV, DPP8, DPP9, and DPP-II by Compounds **9**, **10**, **17**, and **31**


Compd	R ₁	IC ₅₀ (μM) ^a				
		FAP	DPP-IV	DPP8	DPP9	DPP-II
9		0.019	>20	3.7	2.7	>100
10		0.61	>100	>100	>100	>100
17a		0.079	>100	>100	>50	>100
31		0.21	>100	>100	>100	>100
17b		0.066	>100	>100	>50	>100
17c		0.059	>100	>100	>100	>100
17d		0.11	>100	>100	>50	>100
17e		0.088	>100	>100	>100	>100
17f		0.25	>100	>100	>20	>100
17g		0.65	>100	>100	>20	>100
17h		15	>100	>100	>20	>100
17i		0.51	>100	>100	>100	>100
17j		3.2	>100	>100	>100	>100
17k		0.20	>100	>100	>100	>100
17l		0.073	>100	>100	>100	>100
17m		0.73	>100	>100	>100	>100
17n		>20	>100	>100	>100	>100

^aMean values of at least three experiments; standard deviations are ±20%.

Table 3. Inhibition of FAP, DPP-IV, DPP8, DPP9, and DPP-II by Compounds **17–20**, **24**, **27**, **30**, and **32**

Compd	R ₁	R ₂	IC ₅₀ (μM) ^a				
			FAP	DPP-IV	DPP8	DPP9	DPP-II
17a		H	0.079	>100	>100	>50	>100
18a		H	0.020	>100	>100	>50	>100
18b		Cl	0.063	>100	>100	>100	>100
19		H	0.022	>100	>100	>100	>100
24a		H	>50	>100	>100	>100	>100
24b		H	>100	>100	>100	>100	>100
27		H	0.031	0.57	0.50	0.52	0.40
20			>100	>100	>100	>100	>100
32			>100	>100	>100	>100	>100
30			>20	>100	>100	>50	>100

^a Mean values of at least three experiments; standard deviations are $\pm 20\%$.

pyroglutamic acid-based FAP inhibitors were synthesized. As shown in Scheme 2, the fully protected pyroglutamate *trans*-**15** was deprotected by standard hydrogenation condition and was 1-ethyl-3-(3-dimethylaminopropyl)carbodiimide (EDC)-coupled with pyrrolidine derivatives to give *tert*-butyl esters **23** and **25**¹⁷ or followed by dehydration of the amides to give **16**.^{9,35} Removal of the *tert*-butyl protecting group of **16**, **23**, and **25** with trifluoroacetic acid followed by EDC coupling with primary or secondary amines provided the desired (*2S*)-cyanopyrrolidine analogues **17–19**, thiazolidine **24**, and boronic ester **26**, respectively. The free boronic acid **27** was obtained through acid catalyzed transesterification of boronic ester **26** with boron trichloride.¹⁷ The synthesis of *cis*-**31** from *cis*-**15** was identical to that of *trans*-**17** from *trans*-**15**. The proposed mechanism for the formation of byproducts **20–22** is that the nitrile group of **17–19** trapped the *tert*-butyl carbocation followed by hydrolysis to produce amide compounds **20–22**, respectively. Therefore, the search for scavengers of alkylating agents is required. When the thioanisole was used as a scavenger for the intermediate carbocation, its

ability to suppress the formation of **20–22** was not effective. The more promising result was observed when acetonitrile (CH₃CN) was applied as cosolvent with trifluoroacetic acid (TFA), and thus, the nitrile group of CH₃CN participated in the reaction by acting as acceptor of the leaving *tert*-butyl cation. As expected, this approach slashed the yield of **20–22** and produced another byproduct *N*-*tert*-butylacetamide (*M*_w = 115, detected by LC–MS). Compound **30** was prepared in five steps from the known building block **28**, which was synthesized according to literature report (*cis* or *trans* configuration is not assigned).³⁶

Results and Discussion

To establish an optimized P2 site for FAP inhibition, C(4)-substituted pyroglutamic acid based inhibitors with various amines were explored, including bicyclic ring system (**17a–h**), piperazine ring system (**17i,j**), monocyclic system (**17l,m**), and phenylamine (**17n**). These derivatives described above were tested for inhibition of FAP, DPP-IV, DPP8, DPP9, and DPP-II, and the data are summarized in Table 2. Patent search found that

N-acyl-Gly-boroPro **9** is a potent FAP inhibitor with an IC_{50} value of 1.8 nM.³⁷ In our study, the reference compound **9** has an IC_{50} of 19 nM for the inhibition of FAP and is inactive toward DPP-IV and -II (IC_{50} greater than 20 and 100 μ M, respectively), but this compound shows moderate inhibition against DPP8 and DPP9 (3.7 and 2.7 μ M, respectively). A structure–activity relationship (SAR) work was carried out by replacing the boronic acid moiety of **9** with a cyano group. This work has led to the identification of *N*-acyl-Gly-cyanoPro **10** (FAP, IC_{50} = 0.61 μ M), which is 30-fold less potent than **9** and inactive toward the other related enzymes. In the pyroglutamic acid series of compounds, we started initially with the bicyclic system using the isoquinoline ring. Compound **17a** (*trans* configuration) inhibited FAP with an IC_{50} value of 79 nM and inactive toward DPP-IV, DPP-II, DPP8, and DPP9 (IC_{50} > 100 μ M). The *cis* epimer **31** was around 3-fold less potent than *trans*-**17a**. Therefore, a focused structure–activity profiling effort was initiated by modifying the P2 site amine of *trans* isomer **17a**. The introduction of chloro (**17b**), fluoro (**17c**), or trifluoromethyl (**17d**) substituent at the 5-position of the isoindoline gave similar potency (IC_{50} \approx 66–110 nM) compared to **17a**. When the isoindoline moiety of **17a** was replaced with isoquinoline, compound **17e** showed a similar level of FAP inhibition as seen for **17a**. Further modification carried out with heterobicyclic building blocks, such as 4,5,6,7-tetrahydrothieno[2,3-*c*]pyridine **17f**, imidazopyrazine **17g**, and triazolopyrazine derivative **17h**, led to at least a 3-fold decrease in FAP inhibitory potency compared to lead compound **17a**. Compound **17h** is the least potent FAP inhibitor in the bicyclic ring system with an IC_{50} value of 15 μ M.

Replacement of the bicyclic ring system with piperazine derivatives, such as 1-(4-fluorophenyl)piperazine **17i** and 1-pyridin-4-ylpiperazine **17j**, led to no improvement in FAP potency. Among them, the potency of more polar 1-pyridin-4-ylpiperazine **17j** gave a relatively low IC_{50} of 3.2 μ M. On the basis of the results of **17h** (bicyclic system) and **17j** (piperazine system), it seemed that polar substituents at the P2 site would be detrimental to potency; compound **17h** had weak inhibition (IC_{50} > 10 μ M), and compound **17j** exhibited low micromolar activity against FAP. Compound **17k** with a 4-chlorophenyl substituent at the 4-position of 1,2,3,6-tetrahydropyridine is a close analogue of **17i**. This compound showed 2.5-fold more potency than **17i**. As for the effects of monocyclic system, pyrrolidine **17l** (IC_{50} = 73 nM) is equipotent with bicyclic **17a** as FAP inhibitors. However, replacement of the pyrrolidine ring of **17l** with the piperidine (**17m**, IC_{50} = 730 nM) led to a marked 10-fold decrease in potency. Next, when we brought the nitrogen out of the ring system, the aniline **17n** dramatically decreased the inhibitory activity against FAP (IC_{50} > 20 μ M). Therefore, the nitrogen out of the ring system was not further modified. In general, these active FAP inhibitors **17a–n** were inactive toward DPP-IV, DPP8, DPP9, and DPP-II (IC_{50} > 20 μ M).

After optimizing the P2 portion, we turned our attention to the P1 portion of the molecule. The requirements of the S1 pocket for FAP inhibition were explored by keeping isoindoline as the 4-position substituent and varying the 2-position substituent. Their inhibitory properties are shown in Table 3. Incorporation of the (4*S*)-fluoro substituent at the (2*S*)-2-cyanopyrrolidine ring (**18a**, IC_{50} = 20 nM) led to a 4-fold increase in FAP inhibitory activity compared to that of unsubstituted analogue (**17a**, IC_{50} = 79 nM). However, introduction of a chloro substituent at the 5-position of isoindoline

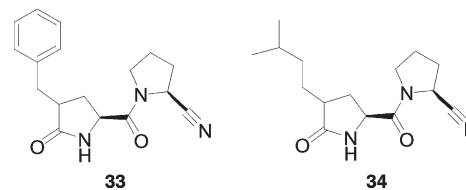


Figure 3. Inactive 4-alkyl substituted pyroglutamic acid amides.

ring (**18b**) showed a decrease in activity (IC_{50} = 63 nM). Compound **19** with a 4,4-difluoro substituent at the 2-cyanopyrrolidine ring exhibited very similar potency to monofluoro substituted **18a**. Changing the 2-position substituent of pyroglutamic acid from 2-cyanopyrrolidine **18a** to thiazolidine **24a** or pyrrolidine **24b** lacking a nitrile moiety showed no significant inhibition toward FAP (IC_{50} > 50 μ M). All of the active FAP inhibitors shown in Table 3 were inactive toward the other related enzymes except boroproline **27**. Even though **27** showed a potent FAP inhibition (IC_{50} = 31 nM), it also exhibited strong inhibitory activity against the other DPP enzymes (IC_{50} values ranged from 400 to 600 nM). So far, from our studies and literature reports, we found that inhibitors of DPPs containing proline boronic acid (boro-Pro) in the P1 site cause poor selectivity of the inhibitors. Compound **20** is a byproduct in the synthesis of compound **17a**. We also investigated the effect of carboxylic acid *tert*-butylamide at the 2-position of pyrrolidine. The bulky amide **20** was inactive against FAP and the other DPP enzymes (IC_{50} > 100 μ M). As for no substituent amide **32** was also inactive toward all the DPP enzymes. It means that dipeptides containing prolineamide in the P1 site cannot be well tolerated by FAP. In comparison with **17a**, 4-carboxypyroglutamic acid diamide **30**, shortened by one carbon at the 4-position of **17a**, caused no significant inhibition against FAP (IC_{50} > 20 μ M) and the other DPP enzymes (IC_{50} > 50 μ M). In addition, we introduced less polar alkyl groups, such as benzyl (**33**) and 3-methylbut-2-enyl (**34**) groups, to replace the 2-(1,3-dihydroisoindol-2-yl)-2-oxoethyl moiety of the lead **17a** at the 4-position of pyroglutamic acid diamide, but none of them showed significant inhibition against FAP (Figure 3, see Supporting Information for details).

Next, we measured the inhibition constant K_i of potent compound **19** against FAP. Assessment of reaction progress curves in the presence of various concentrations of compound **19** revealed a clear, time-dependent approach toward steady state, which is characteristic of slow-binding inhibition kinetics, and the K_i value of **19** is 1.3 nM. In addition, the kinetic mechanism of the inhibition of FAP by the reference compound *N*-acyl-Gly-boroPro **9** was also determined. It showed a competitive inhibition pattern well-fitted to a Lineweaver–Burk plot, and its K_i value was estimated to be 7.9 nM (Figure 4).²⁹

Inhibitors that possessed excellent potency and selectivity profiles were selected for plasma pharmacokinetic screening in mice, and the data are summarized in Table 4. 4-Fluoropyrrolidine derivative **18a** demonstrated short-to-moderate oral half-life (1.8 h), low oral bioavailability (12%), and relatively high clearance (94 (mL/min)/kg). Introducing a 3-chloro substituent at the isoindoline gave compound **18b**, which showed reduction of total body clearance (55 (mL/min)/kg) and prolonged oral half-life ($t_{1/2}$ = 3.6 h) compared to **18a**. On the other hand, although compound **18b** had a very low oral bioavailability (F = 0.7%), it had a very long half-life ($t_{1/2}$ (iv) = 13.3 h) and a favorable drug exposure (AUC) after iv dosing. Therefore, compound **18b** can be selected as an iv route in

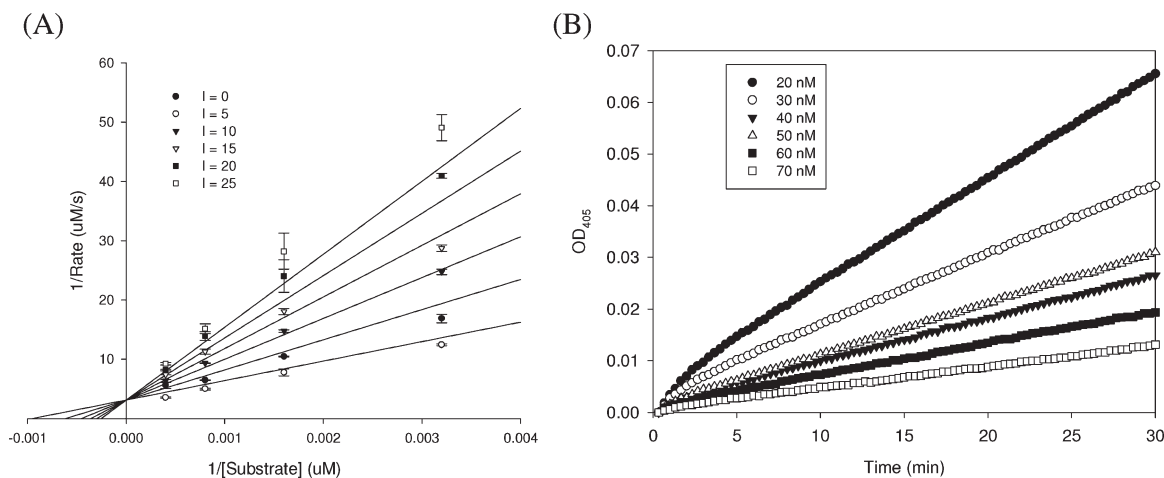


Figure 4. Determination of the K_i values for compounds **9** and **19** against human recombinant FAP (hFAP): (A) competitive inhibition of hFAP by compound **9**; (B) slow-binding kinetics for the inhibition of hFAP by compound **19**. One representative experiment is shown in both panels A and B.

Table 4. Pharmacokinetic Properties of Selected FAP Inhibitors in Mice

compd	intravenous (dose, 2 mg/kg)			oral (dose, 20 mg/kg)			
	CLP (mL/min/kg)	$T_{1/2}$ (h)	AUC (ng/(mL·h))	C_{max} (ng/mL)	$T_{1/2}$ (h)	AUC ng/(mL·h)	F (%)
18a	94	2	460	210	1.8	408	12
18b	58	13.3	593	21	3.6	43	0.7
19	87	0.8	495	108	3.9	336	10

animal models for therapeutic target validation of FAP. The 4,4-difluoropyrrolidine analogue **19** exhibited similar clearance, po AUC, and oral bioavailability to 4-fluoropyrrolidine **18a**. On the contrary, compound **19** showed 2-fold longer oral half-life (3.9 h) and lower C_{max} than **18a** (1.8 h). An analysis of the mouse pharmacokinetic data from the selected FAP inhibitors indicated a strong trend where a more hydrophobic chloro substituent at the isoindoline (**18b**) has a considerably lower plasma clearance and longer half-life after iv dosing and led to a compound with low C_{max} and oral bioavailability after oral dosing.

Conclusions

By introduction of ring-constraint in the lead compound **8** and carrying out SAR studies in a series of substituted 4-carboxymethylpyroglutamic acid diamides, some potent and selective FAP inhibitors have been discovered. Notable among these are compounds **18a** and **19** with a 4-fluoro substituent at the P1 site pyrrolidine ring, which are $IC_{50} = 20$ nM FAP inhibitors with excellent selectivity profile over DPP-IV, DPP-II, DPP8, and DPP9 ($IC_{50} > 50 \mu M$). The SAR suggests that the polar substituents at the P2 site (**17h** and **17j**) would be detrimental to potency and that shortening by one carbon at the 4-position of pyroglutamic acid diamide (**30**) results in a loss in FAP inhibitory potency ($IC_{50} > 20 \mu M$). Our kinetic analyses demonstrated that compound **19** is a slow-binding inhibitor of FAP with K_i value of 1.3 nM. A survey of mouse pharmacokinetic parameters showed that selected compounds **18a,b** and **19** showed poor oral availability in mice. However, **18b** has a longer half-life, lower total body clearance, and favorable drug exposure (AUC) after iv treatment. Thus, compound **18b** can be dosed as iv route to evaluate the potential therapeutic effects of FAP inhibitors in vivo.

Experimental Section

All commercial chemicals and solvents are reagent grade and were used without further treatment unless otherwise noted. 1H

NMR spectra were obtained with a Varian Mercury-300 spectrometer operating at 300 or 400 MHz. Chemical shifts were recorded in parts per million (ppm, δ) and were reported relative to the solvent peak or TMS. High-resolution mass spectra (HRMS) were measured with a Finnigan (MAT-95XL) electron impact (EI) mass spectrometer. LC-MS data were measured on an Agilent MSD-1100 ESI-MS/MS System. Microanalyses were carried out on a Heraeus VarioIII-NCH analyzer. Flash column chromatography was done using silica gel (Merck Kieselgel 60, no. 9385, 230–400 mesh ASTM). Reactions were monitored by TLC using Merck 60 F₂₅₄ silica gel glass backed plates (5 cm \times 10 cm). Zones were detected visually under ultraviolet irradiation (254 nm) or by spraying with phosphomolybdic acid reagent (Aldrich) followed by heating at 80 °C. All starting materials and amines were commercially available unless otherwise indicated. Purity of target compounds were over 95% based on reversed-phase HPLC analyses (Chromolith performance RP-18e 4.6 mm \times 100 mm column) under the two elution conditions. Condition A was 40:60 MeOH–H₂O, and condition B was 70:30 MeOH–H₂O. The flow rate was 0.2 mL/min, and the injection volume was 5 μ L. The system operated at 25 °C. Peaks were detected at $\lambda = 220/254$ nm.

Benzyl (2S,4S)-N-tert-Butoxycarbonyl-4-tert-butoxycarbonylmethylpyrrolidate (trans-15) and Benzyl (2S,4R)-N-tert-Butoxycarbonyl-4-tert-butoxycarbonylmethylpyrrolidate (cis-15). Benzyl (2S)-N-tert-butoxycarbonylpyrrolidate **13**³² (628 mg, 2 mmol) was dissolved in tetrahydrofuran (THF, 10 mL) and cooled to –78 °C, with stirring under nitrogen. LiHMDS (1.0 M in THF, 2.2 mL, 4.4 mmol) was added dropwise over 5 min, and stirring was continued for 1 h. *tert*-Butyl bromoacetate **14** (0.32 mL, 4.0 mmol) was added dropwise over 3 min, and stirring was continued at –78 °C for 2 h. The reaction was quenched with saturated aqueous ammonium chloride and extracted into ethyl acetate. The organic layer was washed with water and saturated aqueous sodium chloride and dried (MgSO₄). The solvent was removed in vacuo to give a brown oil, which was purified by column chromatography on silica gel (eluted with hexane/CH₂Cl₂/EA = 4/5/1) to yield the desired compounds *trans*-**15** (130 mg, 15%) and *cis*-**15** (390 mg, 45%) as white crystalline solids. *trans*-**15**: mp 89–91 °C. $[\alpha]_D^{24} = 24.0$ (*c* 0.2, CH₂Cl₂). 1H NMR (300 MHz, CDCl₃): δ 7.35 (m, 5H), 5.22 and 5.17 (AB quartet, $J = 12.0$ Hz, 2H), 4.62 (dd, $J = 9.6, 1.2$ Hz,

1H), 3.10–2.90 (m, 1H), 2.78 (dd, $J = 17.0, 3.9$ Hz, 1H), 2.39 (dd, $J = 17.0, 8.4$ Hz, 1H), 2.32 (d, $J = 9.0$ Hz, 1H), 2.16–2.02 (m, 1H), 1.42 (s, 9H), 1.40 (s, 9H). MS (ES^+) m/z calcd for $\text{C}_{23}\text{H}_{31}\text{NO}_7$: 433.49. Found: 456.1 ($\text{M} + \text{Na}^+$). *cis*-**15**: mp 70–72 °C. $[\alpha]_{\text{D}}^{24} -15.3$ (c 0.2, CH_2Cl_2). ^1H NMR (400 MHz, CDCl_3): δ 7.36 (m, 5H), 5.22 and 5.17 (AB quartet, $J = 12.0$ Hz, 2H), 4.55 (t, $J = 7.8$ Hz, 1H), 3.05–2.90 (m, 1H), 2.84 (dd, $J = 17.0, 3.9$ Hz, 1H), 2.60–2.70 (m, 1H), 2.34 (dd, $J = 16.7, 10.0$ Hz, 1H), 1.74–1.64 (m, 1H), 1.43 (m, 18H). MS (ES^+) m/z calcd for $\text{C}_{23}\text{H}_{31}\text{NO}_7$: 433.49. Found: 456.2 ($\text{M} + \text{Na}^+$).

Isomerization from *cis*-15 to *trans*-15.³⁴ The *cis*-**15** (433 mg, 1 mmol) was dissolved in CH_2Cl_2 and cooled to 0 °C. DBU (0.44 mL, 3 mmol) was added dropwise and the mixture stirred at 0 °C for 30 min and then at room temperature for 24 h. The mixture was diluted with CH_2Cl_2 and washed once each with 1 N HCl and water. The organic layer was dried over MgSO_4 , filtered, and concentrated in vacuo to give the crude product, which was purified by column chromatography as described above to yield *trans*-**15** (292 mg, 68%) and recovered *cis*-**15** (100 mg, 23%).

General Procedure for the Synthesis of Compounds 16, 23, 25, and 29. To a solution of compound **15** or **28** (1.0 mmol) in MeOH (10 mL) was added 5% palladium on carbon under an atmosphere of nitrogen. The mixture was stirred vigorously under an atmosphere of hydrogen for 5 h at room temperature. The mixture was filtered through Celite and concentrated in vacuo to give (2*S*,4*S*)-*N*-*tert*-butoxycarbonyl-4-*tert*-butoxycarbonylmethylpyrrolidine-1-carboxylic acid or (2*S*,4*S*)-*N*-*tert*-butoxycarbonyl-4-*tert*-butoxycarbonylpyrrolidine-1-carboxylic acid as a pale yellow oil. The crude acid was used for the next reaction without further purification. To a solution containing this acid (343 mg, 1.0 mmol) and *N*-hydroxybenzotriazole (HOBT, 168 mg, 1.1 mmol) in 1,4-dioxane (5 mL) was added a solution of EDC (211 mg, 1.1 mmol) in CH_2Cl_2 (5 mL). The mixture was stirred for 10 min at room temperature. To the resulting solution was added the appropriate proline derivatives (*L*-prolinamide, (2*S*,4*S*)-4-fluoroprolineamide,³⁵ (2*S*)-4,4-difluoroprolineamide,³⁵ thiazolidine or prolineboronic ester,¹⁷ 1.2 equiv) in CH_2Cl_2 (4 mL), with stirring. After 2 h, the reaction mixture was diluted with CH_2Cl_2 and washed with saturated aqueous NaHCO_3 solution (10 mL), 1 N aqueous citric acid solution (10 mL), and brine (10 mL). The combined organic layers were dried over MgSO_4 , filtered, and concentrated. The crude proline amides **16** and **29** and thiazolidine **23** were used for the next reaction without further purification. The crude boronic ester **25** was purified over silica gel using hexane/EA (7:3) as an eluant to yield the desired compound **25** (92%, two steps) as a colorless oil.

To a mixture of the proline amide **16** or **29** (1.6 mmol) and imidazole (0.12 g, 1.8 mmol) in pyridine (5 mL) cooled to –20 °C was added phosphoryl chloride (0.64 g, 4.2 mmol) under nitrogen. After being stirred for 30 min at –20 °C, the mixture was evaporated to dryness in vacuo. The resulting brown solid was dissolved in CH_2Cl_2 (40 mL) and washed with 1.0 N aqueous citric acid (40 mL). The organic phase was dried over magnesium sulfate, filtered, and concentrated under reduced pressure to yield the crude material as a viscous oil. The crude material was purified by chromatography on silica gel (eluted with hexane/EA = 2/1) to give the corresponding nitrile **16** or **29** (>90%) as a white powder. Only the data of representative compounds are shown.

(2*S*,4*S*)-3-*tert*-Butoxycarbonylmethyl-5-((2*S*)-2-cyanopyrrolidine-1-carbonyl)-2-oxopyrrolidine-1-carboxylic Acid *tert*-Butyl Ester (16a**).** Mp 160–162 °C. ^1H NMR (300 MHz, CDCl_3): δ 4.83 (dd, $J = 6.9, 2.1$ Hz, 1H), 4.71 (dd, $J = 9.2, 1.8$ Hz, 1H), 3.79–3.58 (m, 2H), 3.22–3.06 (m, 1H), 2.74 (dd, $J = 17.1, 3.9$ Hz, 1H), 2.50 (dd, $J = 17.0, 8.1$ Hz, 1H), 2.04–2.40 (m, 6H), 1.49 (s, 9H), 1.44 (s, 9H). MS (ES^+) m/z calcd for $\text{C}_{21}\text{H}_{31}\text{N}_3\text{O}_6$: 421.49. Found: 444.1 ($\text{M} + \text{H}^+$), 266.0 ($\text{M} - (\text{Boc})-(\text{tert-butyl}) + \text{H}^+$).

(2*S*,4*S*)-3-*tert*-Butoxycarbonylmethyl-5-((2*S*,4*S*)-2-cyano-4-fluoropyrrolidine-1-carbonyl)-2-oxopyrrolidine-1-carboxylic Acid *tert*-Butyl Ester (16b**).** ^1H NMR (300 MHz, CDCl_3): δ 5.53 (br t,

$J = 3.3$ Hz, 0.5H), 5.38 (br s, 0.5H), 5.04 (d, $J = 9.3$ Hz, 1H), 4.64 (dd, $J = 12.0, 1.5$ Hz, 1H), 4.18–3.83 (m, 2H), 3.20 (m, 1H), 2.78–2.10 (m, 6H), 1.49 (s, 9H), 1.45 (s, 9H).

(3*R*)-3-*tert*-Butoxycarbonylmethyl-2-oxo-5-((2*R*)-2-((1*S*)-2*S*,6*R*,8*S*)-2,9,9-trimethyl-3,5-dioxo-4-bora-tricyclo[6.1.1.0^{2,6}]-dec-4-yl)pyrrolidine-1-carbonylpyrrolidine-1-carboxylic Acid *tert*-Butyl Ester (25**).** ^1H NMR (300 MHz, CDCl_3): δ 4.70 (d, $J = 8.7$ Hz, 1H), 4.27 (dd, $J = 8.7, 1.8$ Hz, 1H), 3.73–3.65 (m, 1H), 3.48–3.40 (m, 1H), 3.29 (dd, $J = 9.0, 7.2$ Hz, 1H), 3.17–3.06 (m, 1H), 2.77 (dd, $J = 16.7, 4.2$ Hz, 1H), 2.42–2.20 (m, 5H), 2.20–1.65 (m, 7H), 1.47 (s, 9H), 1.44 (s, 9H), 1.37 (s, 3H), 1.26 (m, 4H), 0.82 (s, 3H). MS (ES^+) m/z calcd for $\text{C}_{30}\text{H}_{47}\text{BN}_2\text{O}_8$: 574.51. Found: 597.2 ($\text{M} + \text{Na}^+$), 419.1 ($\text{M} - (\text{Boc})-(\text{tert-butyl}) + \text{H}^+$).

5-((2*S*)-2-Cyanopyrrolidine-1-carbonyl)-2-oxo-pyrrolidine-1,3-dicarboxylic Acid di-*tert*-Butyl Ester (29**).** Compound **29** is a single isomer (major). The absolute configuration of **29** at C-4 is not assigned. ^1H NMR (300 MHz, CDCl_3): δ 4.77 (dd, $J = 6.6, 2.1$ Hz, 1H), 4.69 (dd, $J = 9.2, 2.1$ Hz, 1H), 3.73 (td, $J = 9.8, 0.6$ Hz, 1H), 3.72–3.54 (m, 2H), 2.64–2.52 (m, 1H), 2.30–2.03 (m, 5H), 1.43 (s, 15H). MS (ES^+) m/z calcd for $\text{C}_{20}\text{H}_{29}\text{N}_3\text{O}_6$: 407.46. Found: 430.1 ($\text{M} + \text{Na}^+$).

General Procedure for the Synthesis of Compounds 17–19, 20–22, 24, 26, and 30. To a solution of compound **16**, crude **23**, **25**, or **29** (2.0 mmol) in CH_3CN (5 mL) at 0 °C was added TFA (5 mL) dropwise over 5 min. The reaction mixture was stirred for 1 h at room temperature. The reaction mixture was concentrated under vacuum and crystallized with EA/ether to yield the corresponding acids. To a stirred solution of these acids (0.5 mmol) and HOBT (0.55 mmol) in 1,4-dioxane (3 mL) was added a solution of EDC (105 mg, 0.55 mmol) in CH_2Cl_2 (3 mL). The mixture was stirred for 10 min at room temperature. The appropriate 1° or 2° amine (0.55 mmol) in CH_2Cl_2 (2 mL) was added with stirring. After 16 h, the reaction mixture was diluted with CH_2Cl_2 (30 mL) and washed with saturated aqueous NaHCO_3 (30 mL), 1 N aqueous citric acid (30 mL), and brine (30 mL). The organic layers were dried over MgSO_4 , filtered, and concentrated. The residue was purified over silica gel (eluting sequentially with $\text{CH}_2\text{Cl}_2/\text{MeOH} = 98/2, 97/3, 96/4$, and 95/5) to yield compounds **17–19** (75–80%) and byproducts **20–22** (5–10%) from **16**, compound **24** (85%) from **23**, and compound **30** (90%) from **29** as white solids or foam. The elution condition for crude **26** was EA/ $\text{CH}_2\text{Cl}_2 = 1/1$ followed by EtOH/EA/ $\text{CH}_2\text{Cl}_2 = 5/45/50$ to yield **26** (50%) from **25** as a pale brown foam.

(2*S*)-1-((2*S*, 4*S*)-4-[2-(1,3-Dihydroisindol-2-yl)-2-oxoethyl]-5-oxopyrrolidine-2-carbonyl)pyrrolidine-2-carbonitrile (17a**).** Mp 170 °C (dec). ^1H NMR (300 MHz, CDCl_3): (6/1 mixture of *trans/cis* amide rotomers) δ 7.30–7.26 (m, 4H), 6.56 (s, 0.86H), 6.06 (s, 0.14H), 4.82–4.77 (m, overlapped with two singlet at 4.82, 4.77, 4.86H), 4.60 (d, $J = 6.6$ Hz, 0.14H), 4.55 (d, $J = 9.0$ Hz, 0.14H), 4.40 (dd, $J = 3.0, 9.0$ Hz, 0.86H), 3.61–3.04 (m, 2H), 3.02–2.88 (m, 2H), 2.68–2.36 (m, 3H), 2.29–2.12 (m, 4H). MS (ES^+) m/z calcd for $\text{C}_{20}\text{H}_{22}\text{N}_4\text{O}_3$: 366.17. Found: 367.1 ($\text{M} + \text{H}^+$). Anal. Calcd for $\text{C}_{20}\text{H}_{22}\text{N}_4\text{O}_3 \cdot \text{H}_2\text{O}$: C, 62.49; H, 6.29; N, 14.57. Found: C, 62.21; H, 6.14; N, 14.63.

(2*S*)-1-((2*S*,4*S*)-4-[2-(1,3-Dihydroisindol-2-yl)-2-oxoethyl]-5-oxopyrrolidine-2-carbonyl)pyrrolidine-2-carboxylic Acid *tert*-Butylamide (20**).** ^1H NMR (400 MHz, CD_3OD): (2.6/1 mixture of *trans/cis* amide rotomers) δ 8.05 (br s, 0.28H), 7.88 (br s, 0.28H), 7.56 (br s, 0.72H), 7.37–7.28 (m, 4H), 7.21 (br s, 0.72H), 4.90 (s, overlapped with H_2O , 2H), 4.73 (s, 2H), 4.55 (dd, $J = 9.6, 2.8$ Hz, 0.72H), 4.39–4.32 (m, 1H), 4.10 (dd, $J = 8.8, 2.4$ Hz, 0.28H), 3.72–3.50 (m, 2H), 3.05–2.95 (m, 1H), 2.95–2.85 (m, 1H), 2.72–2.28 (m, 3H), 2.18–1.84 (m, 4H), 1.36 (s, 2.52H), 1.32 (s, 6.48H). MS (ES^+) m/z calcd for $\text{C}_{24}\text{H}_{32}\text{N}_4\text{O}_4$: 440.54. Found: 441.2 ($\text{M} + \text{H}^+$). HRMS (FAB) calcd for $\text{C}_{22}\text{H}_{33}\text{N}_4\text{O}_4$: 441.2502. Found: 441.2496.

(2*S*)-1-((2*S*, 4*R*)-4-[2-(1,3-Dihydroisindol-2-yl)-2-oxoethyl]-5-oxopyrrolidine-2-carbonyl)pyrrolidine-2-carbonitrile (31**).** ^1H NMR (400 MHz, CDCl_3): (6/1 mixture of *trans/cis* amide

rotomers) δ 7.29–7.26 (m, 4H), 6.51 (s, 0.86H), 6.24 (s, 0.14H), 4.83–4.74 (m, 5H), 4.59–4.55 (m, 0.14H), 4.40–4.35 (m, 0.86H), 3.69–3.52 (m, 2H), 3.15–3.03 (m, 2H), 2.50–2.38 (m, 1H), 2.31–2.04 (m, 3H), 1.87–1.75 (m, 3H). MS (ES⁺) m/z calcd for C₂₀H₂₂N₄O₃: 366.17. Found: 367.1 (M + H⁺). HRMS (FAB) calcd for C₂₀H₂₂N₄O₃: 366.1692. Found: 366.1691.

(2S)-1-((2S,4S)-4-[2-(5-Chloro-1,3-dihydro-2H-isoindol-2-yl)-2-oxoethyl]-5-oxopyrrolidin-2-yl)carbonylpyrrolidine-2-carbonitrile (17b). ¹H NMR (300 MHz, CDCl₃): (7/1 mixture of *trans/cis* amide rotomers) δ 7.37–7.18 (m, 3.88H), 6.56 (s, 0.12H), 5.31–4.69 (m, 5H), 4.53 (d, J = 9.3 Hz, 0.12H), 4.42 (dd, J = 2.1, 9.3 Hz, 0.88H), 3.61–3.57 (m, 2H), 3.01–2.87 (m, 2H), 2.57–2.18 (m, 7H). MS (ES⁺) m/z calcd for C₂₀H₂₁ClN₄O₃: 400.13. Found: 400.9 (M + H⁺), 402.9 (M + 2 + H⁺).

(2S)-1-((2S,4S)-4-[2-(5-Fluoro-1,3-dihydroisoindol-2-yl)-2-oxoethyl]-5-oxopyrrolidine-2-carbonyl)pyrrolidine-2-carbonitrile (17c). ¹H NMR (400 MHz, CDCl₃): (7/1 mixture of *trans/cis* amide rotomers) δ 7.24–7.19 (m, 1H), 7.02–6.95 (m, 2H), 6.70 (d, J = 4.0 Hz, 0.88H), 6.18 (d, J = 4.0 Hz, 0.12H), 4.83–4.72 (m, 4.88H), 4.61 (d, J = 7.2 Hz, 0.12H), 4.51 (d, J = 8.8 Hz, 0.12H), 4.39 (dd, J = 2.8, 8.8 Hz, 0.88H), 3.69–3.52 (m, 2H), 2.98–2.87 (m, 2H), 2.61–2.39 (m, 3H), 2.30–2.17 (m, 4H). MS (ES⁺) m/z calcd for C₂₀H₂₁FN₄O₃: 384.16. Found: 385.3 (M + H⁺). HRMS (FAB) calcd for C₂₀H₂₂N₄O₃: 366.1692. Found: 366.1691.

(2S)-1-((2S,4S)-4-[2-(5-Trifluoromethyl-1,3-dihydro-2H-isoindol-2-yl)-2-oxoethyl]-5-oxopyrrolidin-2-yl)carbonylpyrrolidine-2-carbonitrile (17d). ¹H NMR (300 MHz, CDCl₃): (7/1 mixture of *trans/cis* amide rotomers) δ 7.60–7.55 (m, 2H), 7.42 (t, J = 7.5 Hz, 1H), 7.19 (d, J = 4.2 Hz, 0.88H), 6.55 (d, J = 4.2 Hz, 0.12H), 4.90–4.83 (m, overlapped two singlet at 4.90, 4.83, 4.88H), 4.69 (d, J = 7.8 Hz, 0.12H), 4.56 (d, J = 8.4 Hz, 0.12H), 4.65 (d, J = 7.8 Hz, 0.88H), 3.64–3.60 (m, 2H), 3.09–2.91 (m, 2H), 2.63–2.20 (m, 7H). MS (ES⁺) m/z calcd for C₂₁H₂₁F₃N₄O₃: 434.16. Found: 435.0 (M + H⁺).

(2S)-1-((2S,4S)-4-[2-(1,3-Dihydro-2H-isoquinol-2-yl)-2-oxoethyl]-5-oxopyrrolidin-2-yl)carbonylpyrrolidine-2-carbonitrile (17e). ¹H NMR (300 MHz, CDCl₃): (7/1 mixture of *trans/cis* amide rotomers) δ 7.28–7.12 (m, 4.88H), 6.54 (s, 0.12H), 4.84 (t like, J = 5.1 Hz, 1H), 4.63 (s, 1H), 4.62 (s, 1H), 4.49 (d, J = 9.3 Hz, 0.12H), 4.38 (d, J = 9.3 Hz, 0.88H), 3.81–3.66 (m, 2H), 3.57–3.53 (m, 2H), 3.00–2.82 (m, 4H), 2.57–2.15 (m, 7H). MS (ES⁺) m/z calcd for C₂₀H₂₄N₄O₃: 380.18. Found: 381.0 (M + H⁺).

(2S)-1-((2S,4S)-4-[2-(6,7-Dihydrothieno[3,2-*c*]pyridine-5(4H)-yl)-2-oxoethyl]-5-oxopyrrolidin-2-yl)carbonylpyrrolidine-2-carbonitrile (17f). ¹H NMR (300 MHz, CDCl₃): (8/1 mixture of *trans/cis* amide rotomers) δ 7.14 (t, J = 5.4 Hz, 1H), 6.88 (d, J = 5.4 Hz, 0.89H), 6.79 (dd, J = 3.3, 5.4 Hz, 1H), 6.43 (d, J = 5.4 Hz, 0.11H), 4.82–4.80 (m, 0.89H), 4.72–4.44 (m, 2.22H, overlapped two singlet at 4.64, 4.56), 4.36 (d, J = 9.6 Hz, 0.89H), 3.96–3.48 (m, 4H), 3.04–2.83 (m, 4H), 2.62–2.11 (m, 5H). MS (ES⁺) m/z calcd for C₁₉H₂₂N₄O₃S: 386.14. Found: 386.9 (M + H⁺). HRMS (FAB) calcd for C₁₉H₂₂N₄O₃S: 386.1413. Found: 386.1411.

(2S)-1-((2S,4S)-5-oxo-4-[2-Oxo-2-(trifluoromethyl)-5,6-dihydroimidazo[1,2-*a*]pyrazin-7(8H)-yl]ethyl]pyrrolidin-2-yl)carbonylpyrrolidine-2-carbonitrile (17g). ¹H NMR (400 MHz, CDCl₃): (6/1 mixture of *trans/cis* amide rotomers) δ 7.22 (d, J = 10.0 Hz, 0.86H), 7.08 (s, 1H), 6.58 (d, J = 10.0 Hz, 0.14H), 4.94–4.57 (m, 3H), 4.47–4.46 (m, 0.14H), 4.32 (d, J = 9.6 Hz, 0.86H), 4.11–3.92 (m, 4H, overlapped singlet at 4.01), 3.61–3.52 (m, 2H), 2.92–2.88 (m, 2H), 2.63–2.54 (m, 1H), 2.42–2.14 (m, 6H). MS (ES⁺) m/z calcd for C₁₉H₂₁F₃N₆O₃: 438.16. Found: 439.1 (M + H⁺). HRMS (FAB) calcd for C₁₉H₂₁F₃N₆O₃: 438.1627. Found: 438.1624.

(2S)-1-((2S,4S)-5-Oxo-4-[2-oxo-2-[3-(trifluoromethyl)-5,6-dihydro[1,2,4]triazolo[4,3-*a*]pyrazin-7(8H)-yl]ethyl]pyrrolidin-2-yl)carbonylpyrrolidine-2-carbonitrile (17h). ¹H NMR (300 MHz, CD₃OD): δ 5.04–4.98 (m, 2H), 4.78 (t, J = 5.4 Hz, 1H), 4.49 (dd, J = 3.0, 8.7 Hz, 1H), 4.35–4.20 (m, 2H), 4.08–4.04 (m, 2H), 3.71–3.57 (m, 2H), 3.04–2.94 (m, 2H), 2.77–2.65 (m, 1H),

2.44–2.05 (m, 6H). MS (ES⁺) m/z calcd for C₁₈H₂₀F₃N₇O₃: 439.16. Found: 440.0 (M + H⁺).

(2S)-1-((2S,4S)-4-[2-[4-(4-Fluorophenyl)piperazin-1-yl]-2-oxoethyl]-5-oxopyrrolidin-2-yl)carbonylpyrrolidine-2-carbonitrile (17i). ¹H NMR (300 MHz, CDCl₃): (7/1 mixture of *trans/cis* amide rotomers) δ 7.27–6.85 (m, 4.88H), 6.27 (s, 0.12H), 4.83–4.82 (m, 0.88H), 4.60 (d, J = 6.6 Hz, 0.12H), 4.48 (d, J = 8.4 Hz, 0.12H), 4.36 (d, J = 8.4 Hz, 0.88H), 3.80–3.55 (m, 6H), 3.10–2.91 (m, 6H), 2.56–2.47 (m, 2H), 2.38–2.17 (m, 7H). MS (ES⁺) m/z calcd for C₂₂H₂₆FN₅O₃: 427.20. Found: 428.0 (M + H⁺).

(2S)-1-((2S,4S)-4-[2-[4-(Pyridine-4-yl)piperazin-1-yl]-2-oxoethyl]-5-oxopyrrolidin-2-yl)carbonylpyrrolidine-2-carbonitrile (17j). ¹H NMR (400 MHz, CDCl₃): (9/1 mixture of *trans/cis* amide rotomers) δ 8.29 (d, J = 5.2 Hz, 2H), 6.95 (s, 0.9H), 6.65 (d, J = 5.2 Hz, 2H), 6.39 (s, 0.1H), 4.82–4.80 (m, 0.9H), 4.60 (d, J = 8.0 Hz, 0.1H), 4.49 (d, J = 8.0 Hz, 0.1H), 4.36 (d, J = 8.0 Hz, 0.9H), 3.85–3.48 (m, 6H), 3.45–3.31 (m, 4H), 3.07–2.87 (m, 2H), 2.55–2.16 (m, 7H). MS (ES⁺) m/z calcd for C₂₁H₂₆N₆O₃: 410.21. Found: 411.3 (M + H⁺), 433.3 (M + 23⁺). HRMS (FAB) calcd for C₂₁H₂₇N₆O₃: 411.2145. Found: 411.2144.

(2S)-1-((2S,4S)-4-[2-[4-(4-Chlorophenyl)-3,6-dihydropyridin-1(2H)-yl]-2-oxoethyl]-5-oxopyrrolidin-2-yl)carbonylpyrrolidine-2-carbonitrile (17k). ¹H NMR (300 MHz, CDCl₃): (9/1 mixture of *trans/cis* amide rotomers) δ 7.30 (s, 4H), 6.80 (d, J = 3.9 Hz, 0.9H), 6.19 (s, 0.1H), 6.06 (br s, 0.5H), 5.99 (brs, 0.5H), 4.83–4.81 (m, 0.9H), 4.60 (d, J = 6.9 Hz, 0.1H), 4.58 (d, J = 9.3 Hz, 0.1H), 4.36 (dd, J = 2.4, 9.3 Hz, 0.9H), 4.20 (brs, 1H), 4.13 (d, J = 2.4 Hz, 1H), 3.82–3.52 (m, 4H), 3.02–2.87 (m, 2H), 2.59–2.46 (m, 4H), 2.39–2.14 (m, 5H). MS (ES⁺) m/z calcd for C₂₃H₂₅ClN₄O₃: 440.16. Found: 440.9 (M + H⁺), 442.0 (M + 2 + H⁺).

(2S)-1-((2S,4S)-5-Oxo-4-[2-oxo-2-(pyrrolidin-1-yl)ethyl]pyrrolidin-2-yl)carbonylpyrrolidine-2-carbonitrile (17l). ¹H NMR (300 MHz, CDCl₃): (13/1 mixture of *trans/cis* amide rotomers) δ 7.41 (s, 0.93H), 6.74 (s, 0.07H), 4.83–4.80 (m, 0.93H), 4.67 (d, J = 4.5 Hz, 0.07H), 4.51 (d, J = 7.8 Hz, 0.07H), 4.42 (d, J = 7.8 Hz, 0.93H), 3.60–3.56 (m, 2H), 3.45–3.39 (q like, J = 6.3 Hz, 4H), 2.95–2.76 (m, 2H), 2.48–2.15 (m, 7H), 1.99–1.80 (m, 4H). MS (ES⁺) m/z calcd for C₁₆H₂₂N₄O₃: 318.17. Found: 319.1 (M + H⁺), 341.1 (M + 23⁺).

(2S)-1-((2S,4S)-5-Oxo-4-(2-oxo-2-(piperidin-1-yl)ethyl)pyrrolidine-2-yl)carbonylpyrrolidine-2-carbonitrile (17m). ¹H NMR (300 MHz, CDCl₃): (8/1 mixture of *trans/cis* amide rotomers) δ 6.72 (s, 0.89H), 6.10 (s, 0.11H), 4.74–4.84 (m, 0.89H), 4.56 (br d, J = 5.7 Hz, 0.11H), 4.45 (br d, J = 7.2 Hz, 0.11H), 4.36 (dd, J = 9.6, 3.0 Hz, 0.89H), 3.76–3.30 (m, 6H), 3.10–2.80 (m, 2H), 2.60–2.00 (m, 7H), 1.74–1.54 (m, 6H). MS (ES⁺) m/z calcd for C₁₇H₂₄N₄O₃: 332.40. Found: 333.1 (M + H⁺). HRMS (FAB) calcd for C₁₇H₂₅N₄O₃: 333.1927. Found: 333.1920.

2-((3S,5S)-5-(((2S)-2-Cyanopyrrolidin-1-yl)carbonyl)-2-oxopyrrolidin-3-yl)-N-phenylacetamide (17n). ¹H NMR (400 MHz, CDCl₃): (8/1 mixture of *trans/cis* amide rotomers) δ 8.96 (s, 1H), 7.54 (d, J = 7.6 Hz, 2H), 7.32–7.15 (m, 2.89H), 7.06 (t, J = 7.6 Hz, 1H), 6.47 (s, 0.11H), 4.75–4.73 (m, 0.89H), 4.61 (d, J = 7.6 Hz, 0.11H), 4.49 (d, J = 8.8 Hz, 0.11H), 4.33 (dd, J = 2.8, 8.8 Hz, 0.89H), 3.50–3.47 (m, 2H), 3.03–2.95 (m, 1H), 2.76 (dd, J = 6.4, 15.2 Hz, 1H), 2.52 (dd, J = 6.4, 15.2 Hz, 1H), 2.40–2.04 (m, 6H). MS (ES⁺) m/z calcd for C₁₈H₂₀N₄O₃: 340.15. Found: 341.0 (M + H⁺). HRMS (FAB) calcd for C₁₈H₂₀N₄O₃: 340.1535. Found: 340.1531.

(2S,4S)-1-((2S,4S)-4-[2-(1,3-Dihydro-2H-isoindol-2-yl)-2-oxoethyl]-5-oxopyrrolidin-2-yl)carbonyl-4-fluoropyrrolidine-2-carbonitrile (18a). Mp 130 °C (dec). ¹H NMR (300 MHz, CDCl₃): (7/1 mixture of *trans/cis* amide rotomers) δ 7.28–7.25 (m, 4H), 7.23 (s, 0.88H), 6.28 (s, 0.12H), 5.54 (br s, 0.44H), 5.46 (br s, 0.06H), 5.36 (br s, 0.44H), 5.30 (br s, 0.06H), 5.09 (d, J = 8.4 Hz, 0.88H), 4.84 (d, J = 8.4 Hz, 0.12H), 4.80 (s, 2H), 4.75 (s, 2H), 4.57 (d, J = 8.4 Hz, 0.12H), 4.38 (d, J = 8.4 Hz, 0.88H), 3.39–3.76 (m, 2H), 3.02–2.78 (m, 2H), 2.67–2.25 (m, 5H). MS (ES⁺) m/z calcd for C₂₀H₂₁FN₄O₃: 384.16. Found: 385.0 (M + H⁺).

Anal. Calcd for $C_{20}H_{21}FN_4O_3 \cdot H_2O$: C, 59.69; H, 5.76; N, 13.92. Found: C, 59.87; H, 5.51; N, 13.84.

(2S,4S)-1-[(2S,4S)-4-[2-(5-Chloro-1,3-dihydroisindol-2-yl)-2-oxoethyl]-5-oxopyrrolidine-2-carbonyl]-4-fluoropyrrolidine-2-carbonitrile (18b). Mp 164–166 °C. 1H NMR (300 MHz, DMSO- d_6): (7/1 mixture of *trans/cis* amide rotomers) δ 8.02 (s, 1H), 7.46 (d, J = 8.4 Hz, 1H), 7.41–7.34 (m, 2H), 5.58 (s, 0.44H), 5.50 (s, 0.06H), 5.46 (s, 0.44H), 5.38 (s, 0.06H), 5.18 (d, J = 8.4 Hz, 0.12 H), 5.05 (d, J = 8.4 Hz, 0.88H), 4.82 (br s, 2H), 4.62 (d, J = 8.8 Hz, 2H), 4.32 (d, J = 8.8 Hz, 0.12H), 4.29 (d, J = 8.8 Hz, 0.88H), 3.89 (br s, 1H), 3.82 (br s, 1H), 2.84–2.62 (m, 2H), 2.52–2.10 (m, 5H). MS (ES^+) m/z calcd for $C_{20}H_{20}ClFN_4O_3$: 418.85. Found: 419.2 (M + H^+), 421.2 (M + 2 + H^+). HRMS (FAB) calcd for $C_{20}H_{20}ClFN_4O_3$: 418.1208. Found: 418.1215.

(2S)-1-[(2S,4S)-4-[2-(1,3-Dihydro-2H-isindol-2-yl)-2-oxoethyl]-5-oxopyrrolidin-2-yl]carbonyl]-4,4-difluoropyrrolidine-2-carbonitrile (19). Mp 156 °C (dec). 1H NMR (300 MHz, DMSO- d_6): (6/1 mixture of *trans/cis* amide rotomers) δ 8.03 (s, 0.86H), 7.97 (s, 0.14H), 7.36–7.25 (m, 4H), 5.37 (d, J = 8.4 Hz, 0.14H), 5.09 (dd, J = 4.2, 8.4 Hz, 0.86H), 4.82 (s, 2H), 4.62 (s, 2H), 4.32 (d, J = 8.7 Hz, 1H), 4.25–4.04 (m, 2H), 2.93–2.66 (m, 4H), 2.49–2.05 (m, 3H). MS (ES^+) m/z calcd for $C_{20}H_{20}F_2N_4O_3$: 402.15. Found: 403.1 (M + H^+). Anal. Calcd for $C_{20}H_{20}F_2N_4O_3 \cdot H_2O$: C, 57.14; H, 5.27; N, 13.33. Found: C, 56.87; H, 5.17; N, 13.43.

(3S,5S)-3-[2-(1,3-Dihydro-2H-isindol-2-yl)-2-oxoethyl]-5-(1,3-thiazolidin-3-ylcarbonyl)pyrrolidin-2-one (24a). 1H NMR (300 MHz, $CDCl_3$): δ 7.30–7.26 (m, 4H), 6.96 (d, J = 10.2 Hz, 1H), 4.82 (s, 2H), 4.77 (s, 2H), 4.66–4.40 (m, 3H), 3.94–3.67 (m, 2H), 3.11 (t, J = 6.3 Hz, 1H), 3.03–2.93 (m, 2H), 2.60–2.46 (m, 2H), 2.40–2.30 (m, 2H). MS (ES^+) m/z calcd for $C_{18}H_{21}N_3O_3S$: 359.13. Found: 360.1 (M + H^+).

(3S,5S)-3-[2-(1,3-Dihydroisindol-2-yl)-2-oxoethyl]-5-(pyrrolidine-1-carbonyl)pyrrolidin-2-one (24b). 1H NMR (400 MHz, $CDCl_3$): δ 7.21–7.18 (m, 4H), 6.51 (s, 1H), 4.71 (d, J = 18.4 Hz, 4H), 4.26 (d, J = 10.0 Hz, 1H), 3.45–3.29 (m, 4H), 2.96–2.85 (m, 2H), 2.50–2.19 (m, 3H), 1.93–1.73 (m, 4H). MS (ES^+) m/z calcd for $C_{19}H_{23}N_3O_3$: 341.40. Found: 342.0 (M + H^+).

(3R)-3-[2-(1,3-Dihydroisindol-2-yl)-2-oxoethyl]-5-(2R)-2-[(1S,2S,6R,8S)-2,9,9-trimethyl-3,5-dioxa-4-bora-tricyclo[6.1.1.0^{2,6}]dec-4-yl]pyrrolidine-1-carbonyl]pyrrolidin-2-one (26). 1H NMR (300 MHz, $CDCl_3$): δ 7.30–7.20 (m, 4H), 5.89 (s, 1H), 4.81 (s, 2H), 4.77 (s, 2H), 4.34 (dd, J = 9.0, 3.0 Hz, 1H), 4.25 (d, J = 9.0 Hz, 1H), 3.55–3.35 (m, 2H), 3.18 (br t, J = 9.0 Hz, 1H), 3.00–2.85 (m, 2H), 2.60–2.45 (m, 2H), 2.45–2.20 (m, 3H), 2.20–1.50 (m, 7H), 1.37 (s, 3H), 1.23 (m, 4H), 0.78 (s, 3H). MS (ES^+) m/z calcd for $C_{29}H_{38}BN_3O_5$: 519.44. Found: 520.2 (M + H^+), 542.2 (M + Na^+).

(2R)-1-[(2S, 4S)-4-[2-(1,3-Dihydroisindol-2-yl)-2-oxoethyl]-5-oxopyrrolidine-2-carbonyl]pyrrolidine-2-boronic Acid (27).

To a stirred solution of BCl_3 (2.5 mL of a 1 M solution in CH_2Cl_2) in CH_2Cl_2 (5 mL) at -78 °C was added (+)-pinanediol [(1R)-1-acetamido-2-(1-naphthyl)ethyl]boronate (**26**, 135 mg, 0.26 mmol). The mixture was stirred at -78 °C for 0.5 h and the cooling bath then removed. The mixture was evaporated under vacuum. Water (30 mL) and Et_2O (70 mL) were added, and the aqueous phase was separated and washed with Et_2O (3×10 mL). Lyophilization of the aqueous phase yielded crude **27**, which was freed from the boric acid contaminant by successive treatments with MeOH (100 mL) followed by distillation until the distillate showed no green boron color in the flame when a drop was ignited. The remaining MeOH was removed by distillation under vacuum. The residue was dissolved in water (10 mL), washed with Et_2O (3×10 mL), and then lyophilized to give **27** (39 mg, 40%) as a pale yellow solid. Mp 100–101 °C. 1H NMR (400 MHz, D_2O): δ (4/1 mixture of *trans/cis* amide rotomers) 7.19–7.17 (m, 4H), 4.69–4.61 (m, 2H), 4.43 (d, J = 6.4 Hz, 0.8H), 4.24 (d, J = 6.4 Hz, 0.2H), 3.65–3.55 (m, 1H), 3.39–3.31 (m, 1H), 3.19 (s, 2H), 3.06–3.02 (m, 1H), 2.91–2.72 (m, 2H), 2.53–2.49 (m, 1H), 2.37–2.21 (m, 2H), 2.01–1.86 (m, 3H), 1.62–1.56 (m, 1H).

(2S)-1-[(2S)-4-(1,3-Dihydroisindole-2-carbonyl)-5-oxopyrrolidine-2-carbonyl]pyrrolidine-2-carbonitrile (30). 1H NMR (300 MHz, $CDCl_3$): δ (major isomer) 7.30–7.21 (m, 4H), 6.86 (br s, 1H), 5.46 (d, J = 6.9 Hz, 1H), 4.94–4.76 (m, 4H), 4.58 (dd, J = 8.6, 5.1 Hz, 1H), 3.85 (dd, J = 9.0, 6.0 Hz, 1H), 3.70–3.56 (m, 2H), 3.16–3.04 (m, 1H), 2.34–2.08 (m, 5H). MS (ES^+) m/z calcd for $C_{19}H_{20}N_4O_3$: 352.39. Found: 353.1 (M + H^+), 375.0 (M + Na^+). HRMS (FAB) calcd for $C_{19}H_{20}N_4O_3$: 352.1535. Found: 352.1536.

(2S)-1-[(2S,4S)-4-[2-(1,3-Dihydroisindol-2-yl)-2-oxoethyl]-5-oxopyrrolidine-2-carbonyl]pyrrolidine-2-carboxylic Acid Amide (32). The title compound was obtained as a white powder in a manner similar to the preparation of **17** except for dehydration step. Mp 150 °C (dec). 1H NMR (400 MHz, CD_3OD): (6/1 mixture of *trans/cis* amide rotomers) δ 7.34–7.28 (m, 4H), 4.91–4.86 (m, overlapped with one singlet at 4.88, 1H), 4.81 (s, 2H), 4.55 (dd, J = 9.4, 2.4 Hz, 1H), 4.50 (dd, J = 8.6, 4.0 Hz, 1H), 3.71–3.60 (m, 2H), 3.04–2.96 (m, 1H), 2.91 (dd, J = 16.6, 4.0 Hz, 1H), 2.65 (dd, J = 16.2, 4.0 Hz, 1H), 2.58–2.50 (m, 1H), 2.40–1.80 (m, 6H). MS (ES^+) m/z calcd for $C_{20}H_{24}N_4O_4$: 384.43. Found: 385.1 (M + H^+). HRMS (FAB) calcd for $C_{20}H_{25}N_4O_4$: 385.1876. Found: 385.1871.

Purification of Human Recombinant FAP, DPP-IV, DPP8, DPP9, and DPP-II from Insect Cells. All the human DPP enzymes used in this study and our previous publications are recombinant proteins expressed individually in insect cells by tagging with His-tag. DPP-IV and DPP8 were expressed and purified as described in our previously published method.^{38–41} Specifically, the purification of DPP9 was carried out with Strep-Tactin resin as we reported previously.⁴² FAP was purified and expressed as described previously.⁵ Specifically, the medium of recombinant FAP from Hi5 insect cells was collected and precipitated by adding 3.8 M ammonium sulfate up to 70% saturation. The pellet was resuspended in the binding buffer containing 20 mM Tris-HCl, pH 8.0, with 500 mM NaCl and bound with the Ni-sepharose (Novagen). After the column was washed with the binding buffer containing 10 and 20 mM imidazole, FAP protein was eluted by 250 mM imidazole. The purification of DPP-II was carried out with modifications by ConA-sepharose and Q-sepharose HP chromatography.⁴³ The culture medium of Hi5 cells expressing DPP-II was collected and adjusted pH to 7.4. It was loaded into ConA-sepharose column and washed with 20 mM Tris, 500 mM NaCl, 1 mM $CaCl_2$, 1 mM $MgCl_2$, pH 7.4. DPP-II was eluted by 250 mM methyl mannopyranoside in 20 mM Tris-HCl, 500 mM NaCl, pH 7.4. The eluent of the ConA-sepharose column was buffer with 20 mM Tris, pH 7.4, with Amicon YM 30 membrane (Millipore). After binding to Q-sepharose HP column, DPP-II was eluted with 0–200 mM NaCl gradient. All the enzymatic preparations have purities of over 90% with a single predominant band on SDS-PAGE gel. Kinetic constants of each batch of the enzymes were measured, and they were similar to the reported values.

IC₅₀ Determination. The enzyme activities were assayed in a total volume of 100 μ L for 30 min at 37 °C at an emission wavelength of 405 nm with Power Wave X spectrometer (Bio-Tek Instrument, Inc., Winooski, VT). The IC₅₀ values for DPP8, DPP9, and FAP were determined in phosphate-buffered saline (PBS, pH 7.4) in the presence of 2.5 mM Gly-Pro-pNA, 1.5 mM Gly-Pro-pNA, and 1.5 mM Ala-Pro-pNA, respectively. The IC₅₀ for DPP-IV was determined in 2 mM Tris-HCl (pH 8.0) in the presence of 500 μ M Gly-Pro-pNA. The IC₅₀ for DPP2 was determined in phosphate buffer (pH 5.5) in the presence of 1.5 mM Gly-Pro-pNA. The inhibitor concentrations ranged from 100 to 0.003 μ M. IC₅₀ values were computed with commercially available curve-fitting programs such as SigmaPlot.

Inhibition Constant (K_i) Measurement. K_i was measured as described previously,²⁹ with a Beckman DU 800 spectrophotometer (Beckman Coulter, Inc., Fullerton, CA). The assays were performed in PBS in a total volume of 100 μ L with 20 nM FAP.

For the competitive binding assays, the substrate concentrations were 312.5–2500 μM and the concentrations of reference compound **9** ranged from 0 to 40 nM. For the slow, tight binding assay of FAP, the concentration of the substrate was 500 μM , and the concentrations of compound **19** ranged from 0 to 70 nM. The hydrolysis of the Ala-Pro-pNA substrate was monitored continuously by measuring the light emission at 405 nm for 30 min. The data were fitted to slow-binding inhibition as previously reported.²⁹ The K_i values are represented as the average of three independent experiments.

Pharmacokinetic Evaluation of the Selected Compounds in Mice. The Balb/c mice for the pharmacokinetic evaluation were obtained from BioLASCO Taiwan Co., Ltd., Ilan, Taiwan, R.O.C., and housed in the animal facility at the National Health Research Institutes, Taiwan, R.O.C. The animal studies were performed according to institutional animal care and committee-approved procedures. Male balb/c mice, each weighing 25–35 g (each 6–8 weeks old), were quarantined for 1 week before use. The animals were fasted before treatment. The selected compounds were given to the groups of mice ($n = 3$ for each time point) as an intravenous (2 mg/kg) or oral (20 mg/kg) dose prepared in a mixture of DMSO/Cremophor/water (5/10/85, v/v/v) by tail-vein injection and orally by gavage. The volume of the dosing solution given was adjusted according to the body weight recorded before the drug was administered. At 0 (immediately before dosing), 2, 5 (intravenous only), 15, and 30 min and 1, 2, 4, 6, 8, 12, and 24 h after dosing, a blood sample was taken from each animal via cardiac puncture and centrifuged at 3000g for 10 min to obtain plasma and then stored at -20°C before analysis. The analyses of the plasma samples were carried out by liquid chromatography–tandem mass spectrometry (LC–MS/MS). The plasma concentration data were analyzed with a standard noncompartmental method with the Kinetica software program (InnaPhase).

Acknowledgment. The study was financially supported by National Health Research Institutes, National Research Program for Genomic Medicine (NRPGM), and National Science Council, Taiwan.

Supporting Information Available: Synthetic scheme and experimental details for the synthesis of compounds **33** and **34** and a figure for recombinant human DPP proteins purified. This material is available free of charge via the Internet at <http://pubs.acs.org>.

References

- Polgar, L. The prolyl oligopeptidase family. *Cell. Mol. Life Sci.* **2002**, *59*, 349–362.
- Rosenblum, J. S.; Kozarich, J. W. Prolyl peptidases: a serine protease subfamily with high potential for drug discovery. *Curr. Opin. Chem. Biol.* **2003**, *7*, 496–504.
- Garin-Chesa, P.; Old, L. J.; Rettig, W. J. Cell surface glycoprotein of reactive stromal fibroblasts as a potential antibody target in human epithelial cancers. *Proc. Natl. Acad. Sci. U.S.A.* **1990**, *87*, 7235–7239.
- Rettig, W. J.; Garin-Chesa, P.; Beresford, H. R.; Oettgen, H. F.; Melamed, M. R.; Old, L. J. Cell-surface glycoproteins of human sarcomas: differential expression in normal and malignant tissues and cultured cells. *Proc. Natl. Acad. Sci. U.S.A.* **1988**, *85*, 3110–3114.
- Aertgeerts, K.; Levin, I.; Shi, L.; Snell, G. P.; Jennings, A.; Prasad, G. S.; Zhang, Y.; Kraus, M. L.; Salakian, S.; Sridhar, V.; Wijnands, R.; Tennant, M. G. Structural and kinetic analysis of the substrate specificity of human fibroblast activation protein α . *J. Biol. Chem.* **2005**, *280*, 19441–19444.
- Cheng, J. D.; Dunbrack, R. L.; Valianou, M.; Rogarto, A.; Aplaugh, R. K.; Weiner, L. M. Promotion of tumor growth by murine fibroblast activation protein, a serine protease, in an animal model. *Cancer Res.* **2002**, *62*, 4767–4772.
- Cheng, J. D.; Valianou, M.; Canutescu, A. A.; Jaffe, E. K.; Lee, H.-O.; Wang, H.; Lai, J. H.; Bachovchin, W. W.; Weiner, L. M. Abrogation of fibroblast activation protein enzymatic activity attenuates tumor growth. *Mol. Cancer Ther.* **2005**, *4*, 351–360.
- Edosada, C. Y.; Quan, C.; Tran, T.; Pham, V.; Wiesmann, C.; Fairbrother, W.; Wolf, B. B. Peptide substrate profiling defines fibroblast activation protein as an endopeptidase of strict Gly(2)-Pro(1)-cleaving specificity. *FEBS Lett.* **2006**, *580*, 1581–1586.
- Villhauer, E. B.; Brinkman, J. A.; Naderi, G. B.; Burke, B. F.; Dunning, B. E.; Prasad, K.; Mangold, B. L.; Russell, M. E.; Hughes, T. E. 1-[[[3-Hydroxy-1-adamantyl]amino]acetyl]-2-cyano-(S)-pyrrolidine: a potent, selective, and orally bioavailable dipeptidyl peptidase IV inhibitor with antihyperglycemic properties. *J. Med. Chem.* **2003**, *46*, 2774–2789.
- Kim, D.; Wang, L.; Beconi, M.; Eiermann, G. J.; Fisher, M. H.; He, H.; Hickey, G. J.; Kowalchick, J. E.; Leitung, B.; Lyons, K.; Marsilio, F.; McCann, M. E.; Patel, R. A.; Petrov, A.; Scapin, G.; Patel, S. B.; Roy, R. S.; Wu, J. K.; Wyrvatt, M. J.; Zhang, B.; Zhu, L.; Thornberry, N. A.; Weber, A. E. (2R)-4-Oxo-4-[3-(trifluoromethyl)-5,6-dihydro[1,2,4]-triazolo[4,3-*g*]pyrazin-7(8H)-yl]-1-(2,4,5-trifluorophenyl)butan-2-amine: a potent, orally active dipeptidyl peptidase IV inhibitor for the treatment of type 2 diabetes. *J. Med. Chem.* **2005**, *48*, 141–151.
- Shrikanth, H. H.; Manojit, P. Medicinal chemistry approaches to the inhibition of dipeptidyl peptidase-4 for the treatment of type 2 diabetes. *Bioorg. Med. Chem.* **2009**, *17*, 1783–1802.
- Senten, K.; Van der Veken, P.; De Meester, I.; Lambeir, A. M.; Scharpé, S.; Haemers, A.; Augustyns, K. Design, synthesis, and SAR of potent and selective dipeptide-derived inhibitors for dipeptidyl peptidases. *J. Med. Chem.* **2003**, *46*, 5005–5014.
- Senten, K.; Van der Veken, P.; De Meester, I.; Lambeir, A. M.; Scharpé, S.; Haemers, A.; Augustyns, K. Gamma-amino-substituted analogues of 1-[(S)-2,4-diaminobutanoyl]piperidine as highly potent and selective dipeptidyl peptidase II inhibitors. *J. Med. Chem.* **2004**, *47*, 2906–2916.
- Jiaang, W. T.; Chen, Y. S.; Tsu, H.; Wu, S. H.; Chien, C. H.; Chang, C. N.; Chang, S. P.; Lee, S. J.; Chen, X. Novel isoindoline compounds for potent and selective inhibition of prolyl dipeptidase DPP8. *Bioorg. Med. Chem. Lett.* **2005**, *15*, 687–691.
- Hu, Y.; Ma, L.; Wu, M.; Wong, M. S.; Li, B.; Corral, S.; Yu, Z.; Nomanbhoy, T.; Alemayehu, S.; Fuller, S. R.; Rosenblum, J. S.; Rozenkrants, N.; Minimo, L. C.; Ripka, W. C.; Szardenings, A. K.; Kozarich, J. W.; Shreder, K. R. Synthesis and structure–activity relationship of *N*-alkyl Gly-boro-Pro inhibitors of DPP4, FAP, and DPP7. *Bioorg. Med. Chem. Lett.* **2005**, *15*, 4239–4242.
- Tran, T.; Quan, C.; Edosada, C. Y.; Mayeda, M.; Wiesmann, C.; Sutherland, D.; Wolf, B. B. Synthesis and structure–activity relationship of *N*-acyl-Gly-, *N*-acyl-Sar- and *N*-blocked-boroPro inhibitors of FAP, DPP4, and POP. *Bioorg. Med. Chem. Lett.* **2007**, *17*, 1438–1442.
- Martichonok, V.; Jones, J. B. Probing the specificity of the serine proteases subtilisin Carlsberg and α -chymotrypsin with enantiomeric 1-acetamido boronic acids. An unexpected reversal of the normal “L”-stereoselectivity preference. *J. Am. Chem. Soc.* **1996**, *118*, 950–958.
- Nauck, M. A.; Wollschlager, D.; Werner, J.; Holst, J. J.; Orskov, C.; Creutzfeldt, W.; Willms, B. Effects of subcutaneous glucagon-like peptide 1 (GLP-1 [7–36 amide]) in patients with NIDDM. *Diabetologia* **1996**, *39*, 1546–1553.
- Drucker, D. J. Biological actions and therapeutic potential of the glucagon-like peptides. *Gastroenterology* **2002**, *122*, 531–544.
- Wettergren, A.; Schjoldager, B.; Mortensen, P. E.; Myhre, J.; Christiansen, J.; Holst, J. J. Truncated GLP-1 (proglucagon 78–107-amide) inhibits gastric and pancreatic functions in man. *Dig. Dis. Sci.* **1993**, *38*, 665–673.
- Nauck, M. A. Is GLP-1 an incretin hormone? *Diabetologia* **1999**, *42*, 373–379.
- Egan, J.; Clocquet, A. R.; Elahi, D. The insulinotropic effect of acute exendin-4-administered to humans: comparison of nondiabetic state to type 2 diabetes. *J. Clin. Endocrinol. Metab.* **2002**, *87*, 1282–1290.
- Gutniak, M.; Orskov, C.; Holst, J. J.; Ahren, B.; Efendic, S. Antidiabetic effect of glucagon-like peptide-1 (7–36) amide in normal subjects and patients with diabetes mellitus. *N. Engl. J. Med.* **1992**, *326*, 1316–1322.
- Gutniak, M. K.; Linde, B.; Holst, J. J.; Efendic, S. Subcutaneous injection of the incretin hormone glucagons-like peptide 1 abolishes postprandial glycemia in NIDDM. *Diabetes Care* **1994**, *17*, 1039–1044.
- Andersen, K. J.; McDonald, J. K. Lysosomal heterogeneity of dipeptidyl peptidase II active on collagen-related peptides. *Renal Physiol. Biochem.* **1989**, *12*, 32–40.
- Mentlein, R.; Struckhoff, G. Purification of two dipeptidyl peptidases II from rat brain and their action on proline-containing neuropeptides. *J. Neurochem.* **1989**, *52*, 1284–1293.

- (27) Abbott, C. A.; Yu, D. M.; Woollatt, E.; Sutherland, G. R.; McCaughan, G. W.; Gorrell, M. D. Cloning, expression and chromosomal localization of a novel human dipeptidyl peptidase (DPP) IV homolog, DPP8. *Eur. J. Biochem.* **2000**, *267*, 6140–6150.
- (28) Lankas, G. R.; Leiting, B.; Roy, R. S.; Eiermann, G. J.; Beconi, M. G.; Biftu, T.; Chan, C. C.; Edmondson, S.; Feeney, W. P.; He, H.; Ippolito, D. E.; Kim, D.; Lyons, K. A.; Ok, H. O.; Patel, R. A.; Petrov, A. N.; Pryor, K. A.; Qian, X.; Reigle, L.; Woods, A.; Wu, J. K.; Zaller, D.; Zhang, X.; Zhu, L.; Weber, A. E.; Thornberry, N. A. Dipeptidyl peptidase IV inhibition for the treatment of type 2 diabetes: potential importance of selectivity over dipeptidyl peptidases 8 and 9. *Diabetes* **2005**, *54*, 2988–2994.
- (29) Wu, J. J.; Tang, H. K.; Yeh, T. K.; Chen, C. M.; Shy, H. S.; Chu, Y. R.; Chien, C. H.; Tsai, T. Y.; Huang, Y. C.; Huang, Y. L.; Huang, C. H.; Tseng, H. Y.; Jiaang, W. T.; Chao, Y. S.; Chen, X. Biochemistry, pharmacokinetics, and toxicology of a potent and selective DPP8/9 inhibitor. *Biochem. Pharmacol.* **2009**, *78*, 203–210.
- (30) Tsai, T. Y.; Hsu, T.; Chen, C. T.; Cheng, J. H.; Chiou, M. C.; Huang, C. H.; Tseng, Y. J.; Yeh, T. K.; Huang, C. Y.; Yeh, K. C.; Huang, Y. W.; Wu, S. H.; Wang, M. H.; Chen, X.; Chao, Y. S.; Jiaang, W. T. Rational design and synthesis of potent and long-lasting glutamic acid-based dipeptidyl peptidase IV inhibitors. *Bioorg. Med. Chem. Lett.* **2009**, *19*, 1908–1912.
- (31) Edosada, C. Y.; Quan, C.; Wiesmann, C.; Tran, T.; Sutherlin, D.; Reynolds, M.; Elliott, J. M.; Raab, H.; Fairbrother, W.; Wolf, B. B. Selective inhibition of fibroblast activation protein protease based on dipeptide substrate specificity. *J. Biol. Chem.* **2006**, *281*, 7437–7444.
- (32) August, R. A.; Khan, J. A.; Moddy, C. A.; Young, D. W. Stereoselective synthesis of (2*S*,4*R*)-[5,5,5-³H₃]leucine. *J. Chem. Soc. Perkin Trans. 1* **1996**, 507–514.
- (33) Carrier, J.-D.; Duffy, J. E. S.; Hitchcock, P. B.; Young, D. W. Usually stereoselectivity in the alkylation of pyroglutamate ester urethanes. *J. Chem. Soc. Perkin Trans. 1* **2001**, 2367–2371.
- (34) Tarver, J. E., Jr.; Terranova, K. M.; Joullie, M. M. Hetero-Diels–Alder and pyroglutamate approaches to (2*S*,4*R*)-2-methyl-amino-5-hydroxy-4-methylpentanoic acid. *Tetrahedron* **2004**, *60*, 10277–10284.
- (35) Fukushima, H.; Hiratate, A.; Takahashi, M.; Saito, M.; Munetomo, E.; Kitano, K.; Saito, H.; Takaoka, Y.; Yamamoto, K. Synthesis and structure–activity relationships of potent 3- or 4-substituted-2-cyanopyrrolidine dipeptidyl peptidase IV inhibitors. *Bioorg. Med. Chem.* **2004**, *12*, 6053–6061.
- (36) Dieltiens, N.; Stevens, C. V.; Masschelein, K. G. R.; Rammeloo, T. [1,2] Boc migration during pyroglutamate alkylations. *Tetrahedron* **2005**, *61*, 6749–6756.
- (37) Bachovchin, W. W.; Lai, H.-S. Inhibitors of Fibroblast Activation Protein Alpha. Patent WO 2007005991 A1, January 11, 2007.
- (38) Chen, Y. S.; Chien, C. H.; Goparaju, C. M.; Hsu, J. T.; Liang, P. H.; Chen, X. Purification and characterization of human prolyl dipeptidase DPP8 in Sf9 insect cells. *Protein Expression Purif.* **2004**, *35*, 142–146.
- (39) Chien, C. H.; Huang, L. H.; Chou, C. Y.; Chen, Y. S.; Han, Y. S.; Chang, G. G.; Liang, P. H.; Chen, X. One site mutation disrupts dimer formation in human DPP-IV proteins. *J. Biol. Chem.* **2004**, *279*, 52338–52345.
- (40) Chien, C. H.; Tsai, C. H.; Lin, C. H.; Chou, C. Y.; Chen, X. Identification of hydrophobic residues critical for DPP-IV dimerization. *Biochemistry* **2006**, *45*, 7006–7012.
- (41) Lee, H. J.; Chen, Y. S.; Chou, C. Y.; Chien, C. H.; Lin, C. H.; Chang, G. G.; Chen, X. Investigation of the dimer interface and substrate specificity of prolyl dipeptidase DPP8. *J. Biol. Chem.* **2006**, *281*, 38653–38662.
- (42) Tang, H. K.; Tang, H. Y.; Hsu, S. C.; Chu, Y. R.; Chien, C. H.; Shu, C. H.; Chen, X. Biochemical properties and expression profile of human prolyl dipeptidase DPP9. *Arch. Biochem. Biophys.* **2009**, *485*, 120–127.
- (43) Leiting, B.; Pryor, K. D.; Wu, J. K.; Marsilio, F.; Patel, R. A.; Craik, C. S.; Ellman, J. A.; Cummings, R. T.; Thornberry, N. A. Catalytic properties and inhibition of proline-specific dipeptidyl peptidases II, IV and VII. *Biochem. J.* **2003**, *371*, 525–532.